DOI: 10.1002/chem.200701103

Sugar–Oligoamides: Bound-State Conformation and DNA Minor-Groove-Binding Description by TR-NOESY and Differential-Frequency Saturation-Transfer-Difference Experiments

Florence Souard,[a] Eva Muñoz,[a] Pablo Peñalver,[a] Concepción Badía,[a] Rafael del Villar-Guerra,[a] Juan Luis Asensio,[a] Jesús Jiménez-Barbero,[b] and Cristina Vicent*[a]

Abstract: Selective-frequency saturation-transfer-difference (STD) spectra allow the description of complexes established between minor-groove binders and long tracts of calf thymus DNA (ct-DNA). Two sets of experiments with selective saturation of either the H1′ or H4′/H5′/H5″ proton NMR regions of deoxyribose allow the description of the ligand residues close to the inner (H1′) and outer regions (H4′/H5′/H5″) of the minor groove of double-helical DNA. A series of complexes of sugar–oligoamides (**2**–**6**) with ct-DNA have been studied by both TR-NOESY and STD experiments. The binding mode of the complexes is similar to that of netropsin (**1**) and allows us to define a general binding mode for this family of ligands, in which an NH rim points towards the internal area (inner region) and a CH_3 rim points towards the external part (outer region) of the minor groove of DNA. Also by means of both TR-NOESY and STD experiments, a description of the asymmetric centers of the sugar residue close to the inner and outer regions of the groove has been achieved. These results confirm that the sugar is responsible for the differences previously found in binding energetics.

Keywords: carbohydrates · conformation analysis · DNA recognition · glycoconjugates · NMR spectroscopy

Introduction

Molecular recognition is at the heart of key biological events. The 3D structures of the molecular complexes formed by ligands and receptors are key factors for the biological response to take place. NMR spectroscopy has made possible the study of the bound-state conformation in solution of a wide range of small ligands bound to biologically relevant macromolecules. In particular, TR-NOESY and ROESY experiments focus on the easily detected NMR signals of the free ligand to gain this information.[1–4] Additionally, description of the epitope of the ligand directly involved in complexation is also possible by using saturation-transfer-difference (STD) experiments.[1,5,6] These two experiments, which are based on intra- or intermolecular magnetization transfer between the ligand and receptor molecules, have been widely used for the description of ligand binding in protein and RNA complexes.[6–14] These macromolecules share the characteristic of highly efficient saturation diffusion, which is typically observed in globular macromolecules.

The use of DNA polymers (calf thymus DNA (ct-DNA), poly(dA–dT)) as a starting point to explore the binding ability of well-known natural DNA binders[15–19] or new designed ligands[20–25] has been essential to determine the binding thermodynamics and the kinetic parameters of the interaction by different techniques, such as fluorescence and microcalorimetry.[26] These DNA polymers of either random or fixed oligonucleotide sequences are helpful models to additionally define the binding selectivity of the ligands for specific DNA sequences.[15,27–30] Thus, these interaction studies

[a] F. Souard, E. Muñoz, P. Peñalver, C. Badía, R. del Villar-Guerra, Dr. J. L. Asensio, Dr. C. Vicent
Departamento de Química Orgánica Biológica
Instituto de Química Orgánica general, CSIC
c/Juan de la Cierva 3, 28006 Madrid (Spain)
Fax: (+34) 91-564-4853
E-mail: iqocv18@iqog.csic.es

[b] Prof. J. Jiménez-Barbero
Dept. of Protein Science
Centro de Investigaciones Biológicas
c/Ramiro de Maetzu 9, 28040 Madrid (Spain)

Supporting information for this article is available on the WWW under http://www.chemeurj.org/ or from the author.

might help in the proper design of short oligonucleotide sequences and, moreover, in obtaining the structural details of the binding mode of the ligand in solution by NMR spectroscopy.

Within a project aimed at the characterization of the basic requirements of the interaction between glycoconjugates and nucleic acids, we have recently designed a vector molecule, the structure of which is made of an oligoamide distamycin-type γ-aminobutyric-linked covalent dimer (Py–γ–Py–Ind; Py: *N*-methylpyrrole; γ: γ-aminobutyric linker; Ind: indole), to study its binding ability with DNA by using fluorescence spectroscopy. DNA polymers (ct-DNA, poly(dA–dT), and poly(dC–dG)) were employed. This method allowed the selectivity of the vector molecule for ATAT sequences to be determined.[31]

Additionally, we have also shown, again by using fluorescence methods, that the vector can be used as a sugar carrier to the minor groove of DNA (Scheme 1). Initially NMR[32] and fluorescence studies[31] suggested that the previously synthesized sugar–oligoamides **2**, **4**, and **5** presented a noticeable percentage of hairpin conformation in the free state, which was kept upon DNA binding. Also, competition NMR experiments suggested that the designed ligands are minor-groove binders.[32] Thus, at least for the initial designed molecules, the sugar residue seems to modulate the binding for the different DNA polymers studied and, even more relevantly, *the sugar contributes to the selectivity of binding.*

From a detailed structural perspective, and with regard to the description of the complexes formed by long tracts of helical DNA (DNA polymers) with small ligands, the definition of the molecular-recognition process at the structural level has been elusive, due to the intrinsic difficulties of using the proper techniques (such as NMR experiments) in these complex systems.

On this basis, we herein present nonambiguous NMR evidence of the molecular-recognition ability of the previously studied (**2**, **4**, and **5**)[32] and new sugar–oligoamides (**3** and **6**) towards DNA sequences and provide additional tools, also based on recently proposed STD-based NMR experiments,[33] to study this interaction at atomic resolution.

Results and Discussion

The understanding of the recognition features of **2**–**6** (see Scheme 1) with respect to DNA requires a proper understanding of the conformational properties of these molecules in both the free and bound states. Thus, we aimed to get experimental evidence that could be related to the sugar proximity to the DNA grooves. Additionally, knowledge of the disposition of the pyranose moiety relative to either the inner or the outer region of the DNA minor groove could be used for further design within the sugar and/or the vector part of the ligand.

On this basis, STD experiments were employed to get information on the ligand epitope with long tracts of helical DNA. Recently, Gomez-Paloma and co-workers have described the differential-frequency STD experiment as a tool to distinguish between the three main different DNA–ligand binding modes: minor groove, external electrostatic, and intercalative binding.[33] For this particular recognition process, the difference in the vertical and horizontal dimensions of the macromolecule generates an anisotropy that renders different efficiencies of saturation diffusion along the two axes, thereby making the STD experiment different to that used for other biomolecules. This important anisotropic effect in saturation diffusion also generates different experimental outcomes depending on the chosen saturation frequency (and, therefore, the DNA region).

The structure of the minor groove of B-DNA is characterized by the presence of the sugar deoxyribose in the phosphodiester backbone, and the attachment of the bases to the backbone sugars through the glycosidic bonds is asymmetrical. This fact results in the formation of two different grooves, the major and minor grooves,

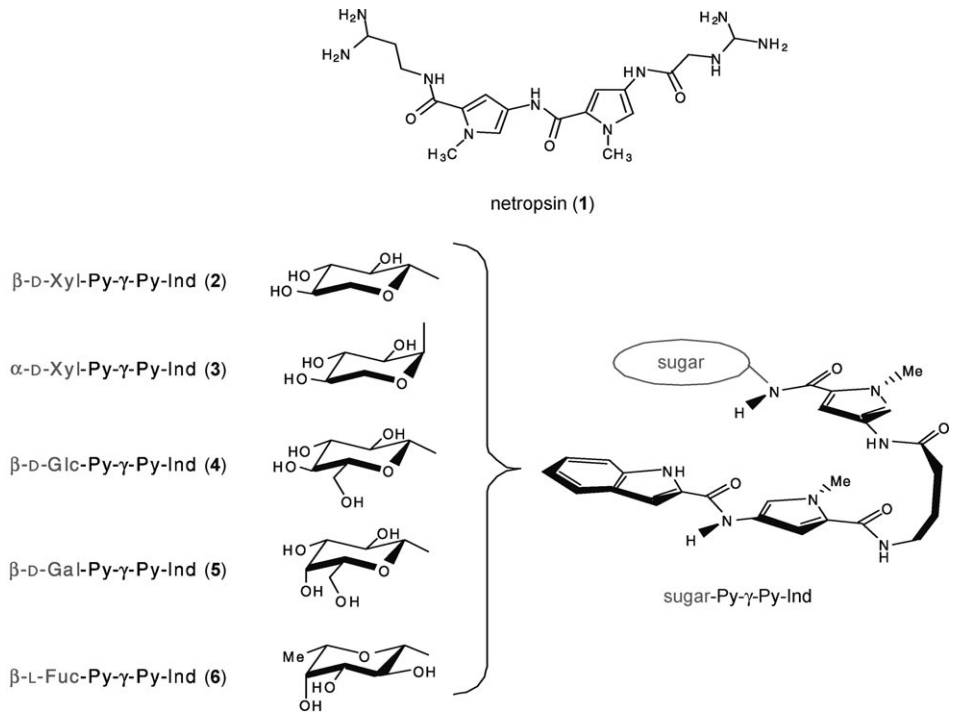

Scheme 1. Netropsin (**1**) and sugar–oligoamides (**2**–**6**). Xyl: xylose; Glc: glucose; Gal: galactose; Fuc: fucose.

on opposite sides of the base pairs. The floors of the grooves serve as recognition sites for interacting molecules through hydrogen-bonding centers. The binding of small molecules is expected to give close contacts with the internal and external regions of the groove, always depending on the structure of the ligand and on the width of the groove. Nevertheless, this last feature varies depending on the specific oligonucleotide sequence at the DNA binding site. With regard to the location of the deoxyribose hydrogen atoms attached to the asymmetric carbon atoms within the groove structure, inspection of a B-DNA model (see Figure 1) indicates that hydrogen atom H1′ is closer to the internal region of the groove, while hydrogen atoms H4′, H5′, and H5″ are directed towards the external area.

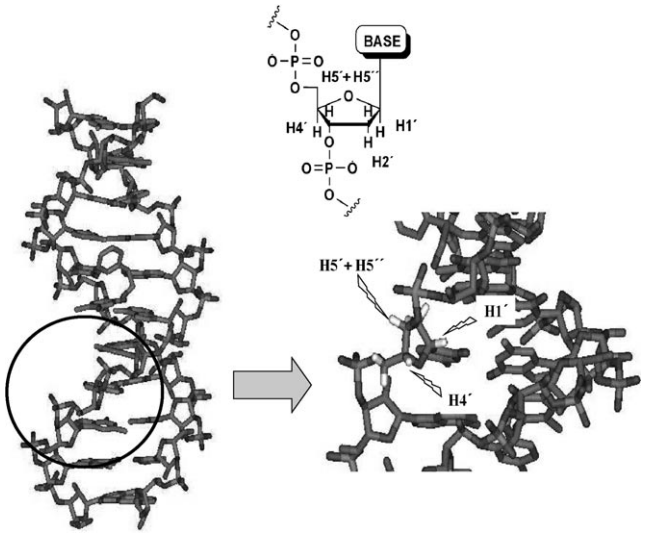

Figure 1. X-ray crystal structure of B-DNA, with identification of the positions of H1′, H4′, H5′, and H5″ of the deoxyribose ring within the double helix.

Thus, we decided to explore the use of the anisotropic effect in saturation diffusion found in the STD experiment for our minor-groove ligands (**2**–**6**).

Hence, two parallel sets of STD experiments were performed under the same experimental conditions, with only variations in the position at which saturation was elicited. Irradiations were selected by choosing suitable frequencies from the specific DNA regions, either H1′ at $\delta = 5.6$ ppm (internal-minor-groove region) or H4′, H5′, and H5″ at $\delta =$ 4.5 ppm (external-minor-groove region, Figure 2).[34] In all cases, off-resonance irradiation was set at $\delta = 50$ ppm. A careful comparative analysis of the observed effects for the two STD sets was then performed.

It is well known[6] that the percentage of saturation transfer from the DNA protons to the ligand protons essentially depends on the saturation time, the dissociation rate, and the molar fractions of the bound and free ligand. In general, if the time of saturation is too short, the transfer of saturation will be not efficient enough and the signal/noise ratio will be too small to clearly identify the bound epitopes. On the other hand, if it is too long, the magnetization could be transferred throughout the entire bound molecule by spin diffusion. Thus, after carefully checking for spin-diffusion effects, we decided to employ a relatively short saturation time of 400 ms for the study of all DNA-bound sugar–oligoamides.

As a first step, netropsin (**1**)[35] was used to validate the method as its binding mode to ct-DNA has been very well established. The two sets of STD experiments for the **1**–ct-DNA complex by selective saturation on H1′ (in) or H4′/H5′/H5″ (out)[36] gave a general clear-cut trend that could be related to the location of the different protons of the ligands in the DNA binding site (see Figure 4). While H1′ saturation gave a significant enhancement of the resonances assigned to Py3A and Py3B (in red), the transfer of saturation from H4′/H5′/H5″ rendered a major enhancement on CH_3A, CH_3B, P5A, and P5B (in blue). For netropsin labeling and STD results, see Table 1 in the Supporting Information. These observations are in agreement with a crescent conformation of netropsin in the bound state, for which the methyl groups of the pyrrole amino acids and Py5 are directed towards the outer region of the groove, while Py3A and Py3B are pointing towards the inner region (Figure 2).

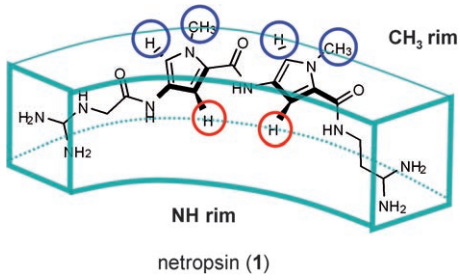

Figure 2. STD results for the netropsin–ct-DNA complex.

Interestingly, this conformation is completely in accordance with that described for the bound state of netropsin in the 1:1 complexes formed with several dodecanucleotides in solution[37,38] and in the solid state.[39–45] Hence, the differential-frequency STD experiment is providing valuable geometric information on the bound state of this minor-groove binder. In this particular case, the NH rim is directed toward the inner side of the minor groove, while the CH_3 rim of the ligand is pointing towards the outer side of the minor groove.

Thus, once the method was validated, our target sugar–oligoamides (**2**–**6**; Scheme 1) were studied.

However, if the STD method is to be used, obviously, the careful evaluation of the STD-based structure information for the complexes between **2**–**6** and ct-DNA needs to be sustained by previous knowledge of the free- and bound-state conformations of these sugar–oligoamides with ct-DNA.

With regard to the free state, we have previously reported that **2**, **4**, and **5** adopt major hairpin-like conformations in the free state.[32] For this geometry, an NH rim and a CH_3 rim (see Figure 4) can be safely defined. For the new molecules **3** (α anomer of xylose) and **6** (β-L-Fuc), Figure 3a shows the key interstrand NOEs found. The results show that neither the α/β nor the D/L series seems to alter the presence of a crescent hairpin conformation in the free state in a significant manner(See the discussion below and the Supporting Information).

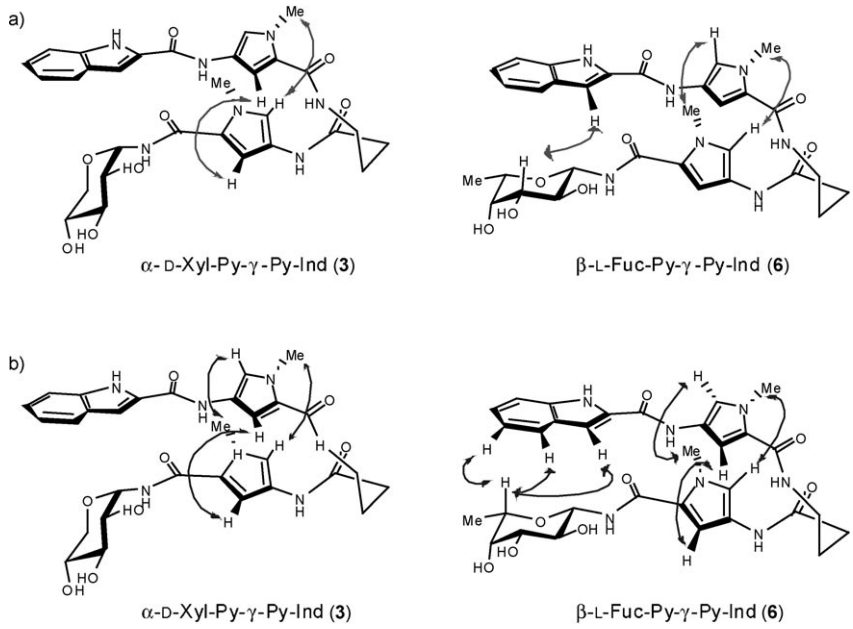

Figure 3. a) Interstrand NOEs for sugar–oligoamides **3** and **6** in the free state. b) Interstrand NOEs for sugar–oligoamides **3** and **6** in the bound state.

Just as additional experimental data, and for sake of clarity, a general discussion of the coupling constant values (J^3_{NH5-H1}) related to the conformation around the glycosidic linkages (see Table 3 in the Supporting Information) will be given here. For **2** and **4–6**, the observed values are between 9.2–8.5 Hz. There is not any particular Karplus equation for this particular arrangement of H1–C1–N–H5, in which the C1 atom is substituted by both oxygen and carbon atoms and the nitrogen atom holds a carbonyl group. The most similar equation has been recently reported, but it only accounts for acetamide sugars at position C2 and not at C1.[46] Nevertheless, according to previous observations in glycosyl amides,[47] these values are in agreement with a major *trans* orientation of NH5 and the H1 atom of the sugar pyranose ring. Moreover, an NH5–H2 NOE was detected in these cases, clearly supporting the predominant contribution of the *anti* conformer, which allows a quasiparallel orientation between the plane defined by the sugar pyranose and the indole ring.

By contrast, for the α-D-Xyl analogue, **3**, the J_{NH5-H1} value (7.7 Hz) is significantly smaller and indicates the presence of a mixture of conformers in solution around the glycosidic linkage. As a matter of fact, no NOE (either NH5–H1 or NH5–H2) was detected that could support a major conformer in solution. Thus, at least at the glycosidic linkage level, **3** behaves differently to **2** and **4–6**, for which major *anti* conformers were present.

The hairpin-like conformation of the oligoamides is defined by a set of NOEs between the indole-strand and sugar-strand moieties joined by the γ-aminobutyric fragment: in particular, the CH_3A/Py5B and Py3A/Py3B proton pairs. This geometry is further clarified by a set of additional NOEs between some pyranose and indole protons.

Indeed, for the β-L-Fuc analogue, **6**, both sets of CH_3A/Py5B and Py3A/Py3B were found (Figure 3) and, moreover, an interstrand NOE between the H3 atom of the fucopyranose ring and the In3 atom of the indole allowed us to conclude that, in this case, the α face of the sugar is pointing towards the indole ring in the free state (Figure 3). A different trend was observed for **3**. In this case, the interstrand NOEs corresponding to the oligoamide fragment (Py5A/CH_3B and Py5B/CH_3A) were detected, but no NOEs between the indole and sugar proton resonances were found. Although negative NOE data should not be taken as a major source for conclusions, this observation is in agreement with the coupling-constant data supporting a different shape for **3** to that for the rest of the analogues (Figure 3a). The α-anomeric geometry places the sugar out of the plane of the oligoamide, while, for instance, for the β-D-Xyl derivative **2**, the β face of the xylopyranose ring is close to the indole ring.[32] Nevertheless, in both **2** and **3**, the crescent-shaped hairpin conformation is present in aqueous solution, as deduced from the Py5A/CH_3B and Py5B/CH_3A NOEs.

Thus, ligands **2–6** adopt a significant percentage of a crescent-shaped folded conformation in the free state, for which NH and CH_3 rims can be defined (see Figure 4).

With regard to the bound-state conformation in the ct-DNA complexes, as mentioned above, this knowledge has been previously deduced for **2**, **4**, and **5** based on TR-NOESY data. Thus, on this basis, we carried out the first TR-NOESY experiments for the new sugar–oligoamides (**3** and **6**) in the presence of ct-DNA. For the β-L-Fuc analogue **6**, TR-NOESY experiments were carried out in H_2O and D_2O to obtain NOEs from both exchangeable (amide) and nonexchangeable protons (see the Supporting Information).

The representation in Figure 3b exemplifies the interstrand NOEs detected in the TR-NOESY experiments for **3** and **6** in the presence of ct-DNA. The complexes of both **3** and **6** with ct-DNA present interstrand NOEs between CH_3A/Py5B and CH_3B/Py5A. The complex of **6** also shows the P3A/P3B NOE and, more importantly, the $H5_{ax}$ proton of the fucopyranose moiety shows NOEs with the resonances of In3, In4 and In5 on the indole ring. Hence, for **6**, the TR-NOESY spectrum of the complex with ct-DNA does not only show the interstrand contacts for the vector-oligoamide fragment (crescent hairpin conformation) but additionally permits confirmation of the spatial proximity between the α face of the sugar ring and the indole residue in the bound state. In the case of the α-D-Xyl derivative **3**, as observed in the free state, no NOEs were found between the sugar and the indole moiety in the bound state. In both cases, all of these negative TR-NOE cross-peaks confirmed the presence of the hairpin conformation in the bound state.

The observed inter- and intrastrand NOEs (see the Supporting Information) conclusively prove that the change from a β to an α linkage or from the D to L series of the sugar residues does not strongly affect the presence of a crescent-shaped folded conformation in the ct-DNA bound state. However, the relative orientation of the sugar with respect to the rest of the oligoamide chain is clearly perturbed when passing from equatorial (**2**, **4**–**6**) to axial (**3**) anomers. Nevertheless, according to the hairpin-like conformation, NH and CH_3 rims can be defined (see Figure 4).

Once the bound-state geometry had been deduced, the next step was to perform the differential-frequency STD experiments for the complexes formed by **2**–**6** and ct-DNA. Here, as for the **1**–ct-DNA complex described above, two parallel sets of STD experiments were performed for each complex under the same experimental conditions.

Figure 4 shows, in blue, the resonances of the ligands that are enhanced by irradiating the H4′/H5′/H5″ spectral region. As mentioned above, these sets of experiments allow the ligand epitope close to the outer region of the DNA groove to be described. On the other hand, the resonances of the ligand in proximity with the inner region of the minor groove (enhanced by irradiating H1′) are shown in red. The obtained results suggest that the binding mode of these γ-linked covalent dimers (**2**–**6**) places their NH-rim areas close to the inner region of the ct-DNA minor groove (Py3A and Py3B are enhanced when H1′ is saturated). Moreover, the CH_3 rim is close to the outer region of the groove (CH_3A, CH_3B, Py5A, and Py5B are enhanced when H4′/H5′/H5″ are saturated). These results, which are in perfect accordance with those obtained for netropsin (**1**), resemble the hairpin conformation with a crescent structure, which was also determined by NMR spectroscopy, in complex aromatic oligoamide ligands bound to short DNA fragments.[48–50]

Enhancement on the sugar region could only be interpreted on a qualitative basis since strong signal overlap, as well as spin diffusion along the pyranose protons, precluded the derivation of clear-cut structure information for the relative orientation of these protons in most of the cases. Nevertheless, this constitutes a significant result. Saturation is transferred from the ct-DNA to the sugar residues for all of the sugar–oligoamide/ct-DNA complexes. Thus, even under these conditions, the STD experiment constitutes a relevant experimental demonstration of the proximity of the sugar to the minor groove and confirms that the designed vector-oligoamide molecule, Py–γ–Py–Ind, allows sugars to be carried to the minor groove of B-DNA.

In any case, the consideration of the bound-state conformation (as deduced from the TR-NOESY data) with the

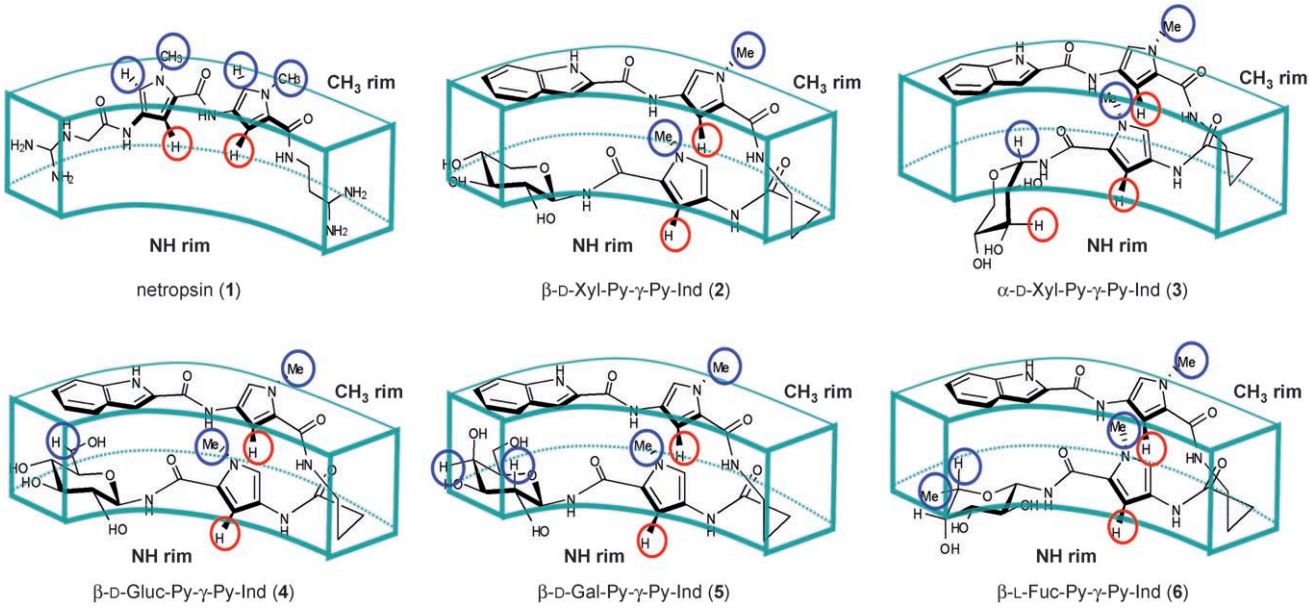

Figure 4. STD results for the complexes of netropsin (**1**) and sugar–oligoamides **2**–**6** with ct-DNA.

proximity of either the NH or CH_3 rim to the groove of ct-DNA (as determined from STD data) permitted the formation of a general idea of the global orientation of the sugar–oligoamide in the DNA. Indeed, although only the STD results obtained for the β-L-Fuc analogue **6** (Figure 4) could be clearly assessed, the small observed overlapping for the key Fuc protons allowed a well-defined binding mode to be proposed. The differential-frequency STD enhancements permitted us to deduce that C5 (CH_3, H5) and C4 (H4) are pointing toward the outer region of the groove, with the α face of the fucose moiety pointing toward the indole ring in the hairpin structure, as already characterized by the TR-NOESY results.

Thus, the results obtained herein have shown a general trend regarding the orientation of the oligoamide fragment of all of the sugar–oligoamides studied (**2–6**). The most significant result is that neither the α or β linkage of the sugar to the oligoamide or the intrinsic features of the sugar residue (different axial or equatorial substituents, D or L series) strongly modify the position of the oligoamide Py–γ–Py–Ind vector within the groove of the B-DNA.

Therefore, based on TR-NOESY and STD experiments, the sugar–oligoamides **2–6** when bound to ct-DNA adopted a crescent-shaped folded conformation in which the NH rim is directed toward the inner region of the minor groove, while the CH_3 rim is directed toward the outer region, a binding mode similar to that of the netropsin–ct-DNA complex.

Conclusion

Differential-frequency STD experiments have been used as a major tool to characterize the key structural features of small minor-groove binders with long tracts of DNA in solution. Selective saturation at different spectral regions can be used as a fingerprint trace to locate the residues from the bound ligand close to the inside or outside areas of the groove. Thus, the combination of STD and TR-NOESY experiments has allowed the determination of the conformation of **2–6** in the bound state, as well as their binding modes in the groove of ct-DNA. Moreover, this method has unequivocally assessed the spatial proximity between the sugar residue and the groove. We feel that this experiment, as originally proposed by Gomez-Paloma and co-workers,[33] is indeed an adequate means to study the binding ability of ligands to DNA chains.

Thus, with all this new structure information at hand, it is now possible to strongly support the theory that the previously reported differences in binding energetics[31] for the sugar–oligoamides (**2–6**) with ct-DNA depend on the chemical nature of the sugar residue ($\Delta\Delta G°$ **5** (poly(dA–dT)−ct-DNA) = −4.0 kcal mol^{-1}; $\Delta\Delta G°$ **2** (poly(dA–dT)−ct-DNA) = −1.5 kcal mol^{-1}).

On this basis, it is shown that the different sugars interact differently with the DNA, possibly due to the different amphiphilic character of their surfaces. This new knowledge is helpful to us in the rational design of potent multivalent DNA binders.

Experimental Section

Solvents were purified according to standard procedures. NMR spectroscopic measurements were recorded on a Bruker AVANCE 500 MHz spectrometer. Calf thymus DNA (ct-DNA) was purchased from Sigma and used without further purification. H_2O for NMR studies was freshly filtered milli-Q water. Netropsin was purchased from Fluka (lot no. 405625-1) and used without further purification. Sugar–oligoamides (**2–6**) were synthesized according to the procedure previously described for β-Gal-, β-Glc-, and β-Xyl-Py-γ-Py-Ind (see Figure 23 in the Supporting Information).[32]

Structural studies:

^{1}H NMR experiments with ligands 1–6: All spectra in aqueous solution were recorded with presaturation of the water signal. The chemical shifts were reported in ppm relative to 2,2-dimethyl-2-silapentane-5-sulfonic acid or trimethylsilylpropionic acid (0.00 ppm) when D_2O was used and relative to residual acetone (2.04 ppm) when D_2O/[D_6]acetone or H_2O/[D_6]acetone were used in the experiment. NMR structural studies of compounds **1–6** were based on monodimensional and bidimensional (TOCSY, HSQC, NOESY, ROESY) experiments and were recorded at 400 or 500 MHz and 26 °C in a Varian instrument. Sample solutions were prepared at concentrations ranging between 2 and 0.1 mM depending on the solubility of the compounds.

Bound-state NMR spectroscopic experiments (TR-NOESY and differential-frequency STD): These experiments were carried out in phosphate buffer (10 mM, pH 7). Ligand samples were prepared at a constant concentration of 1 mM. The ct-DNA titrant sample (stock solution) was prepared by dissolving ct-DNA (2 mg) in a 1 mM solution of ligand (1 mL). The concentration of ct-DNA was calculated by UV/Vis spectroscopy ($c = 2.51 \times 10^{-3}$ M, $\varepsilon = 13\,200$ M^{-1}cm^{-1}).[51,52] The NMR spectroscopic sample was prepared by titration of the ligand solution (0.6 mL) with increasing amounts of the titrant DNA solution, with the ligand concentration kept constant. A 1D NMR spectrum was recorded in the same "acquisition mode" (no. of scans = 256, T = 26 °C) after each addition of ct-DNA. A progressive broadening and disappearance of the proton signals from the ligand was observed; this indicates binding of the ligand to ct-DNA. The bound-state NMR experiments were carried out once the spectra of the free ligand was clear but slightly broadened (addition of ct-DNA: 100 μL for β-D-Glc and β-D-Gal derivatives **4** and **5**, 140 μL for β-L-Fuc analogue **6**, 170 μL for netropsin (**1**), 425 μL for α-d-Xyl derivative **3**). The same NMR tube was used for both the TR-NOESY and STD experiments in every case.

TR-NOESY experiments: TR-NOESY experiments for the bound ligand were performed on 500 MHz spectrometers (Varian or Bruker) with saturation of the residual H_2O signal or with the Watergate pulse sequence. TR-NOESY experiments were recorded at 26 °C and performed with mixing times of 200, 300, and 400 ms. The experiments in H_2O/15 % D_2O were recorded at 18 °C to minimize the hydrogen/deuterium exchange.

Negative and intense NOEs (which are indicative of binding to the macromolecule) were found in all of the experiments; these were in contrast with the weak NOEs (typical of small molecules) observed in the free-state conformation for all of our oligoamides (**2–6**).

STD experiments: STD experiments for the bound ligands were performed on a 500 MHz AVANCE Bruker spectrometer. In the case of the samples in H_2O, the Watergate pulse sequence was used. In the case of the samples in D_2O, either no water suppression or the Watergate sequence was used depending on the obtained signal/noise ratio without solvent suppression. A ligand/receptor molar excess of up to 2.8:1 for β-D-Glc and β-D-Gal analogues **4** and **5** was used for the best STD effects. The STD effects of the individual protons were calculated for each compound relative to a reference spectrum with off-resonance saturation at δ = 50 ppm. 128 scans were recorded for the reference STD spectrum.

The best duration of the saturation pulse, the power of the selective Gaussian pulse, and the recycling delay were optimized to get the best possible signal/noise ratio with no spin diffusion within a reasonable experimental time. The final experiments were performed at 298 K with a recycling delay of 4 s, an acquisition time of around 1.3 s, and a saturation time of 400 ms. The saturation was accomplished by using 8 Gaussian shaped pulses of 49 ms each, separated by 1 ms, with an approximate power of $\gamma B = 20$ Hz. Two saturation frequencies were selected: $\delta =$ 4.50 ppm (to hit the H_4', H_5', and H_5'' region of deoxyribose in DNA) and $\delta = 5.60$ ppm (to hit the H1′ region in DNA). The closest proton resonances of the ligand were the anomeric proton of **6**, at $\delta = 4.75$ ppm, and the Py3A hydrogen atom at $\delta = 6.46$ ppm. Blank experiments performed without the DNA receptor showed that no effect was observed in the ligand protons when the H1′ region ($\delta = 5.60$ ppm) in DNA was chosen, while less than 5% saturation was observed in the anomeric H1 resonance of compound **6** for on-resonance saturation at $\delta = 4.50$ ppm. Although this minor saturation does not imply any major concern in the actual STD experiments and does not affect the vicinal protons through spin diffusion, no STD effects in the sugar moiety of **6** were considered.

The intensity of each peak in the STD spectra was standardized in relation to a proton resonance the intensity of which was assigned to be 100. The normalization of the signal intensity was done relative to Py3 and Py5. Both sets of data treatment rendered identical conclusions. Such conclusions were obtained by comparing the normalized value of each proton resonance intensity upon irradiation of the outer or inner region of the DNA groove. (A proton is thought to be closer to the irradiated region of DNA when a bigger normalized intensity value is obtained if the difference in percentage between both regions of DNA is at least 10–15%.)

Acknowledgements

Financial support for this work was provided by the MEC (BQU2003-03550-C03-01 and -02 and CTQ2006-10874-C02-01 and -02) and a European RTN project (HPRN-CT-2002-00190). P.P. is grateful to the Consejo superior de Investigaciones Científicas for an I3P predoctoral fellowship. C.B. and R.V.-G. thank the MEC for FPI and FPU predoctoral fellowships, respectively, while F.S. thanks RTN for a postdoctoral position.

[1] M. Vogtherr, T. Peters, *J. Am. Chem. Soc.* **2000**, *122*, 6093–6099.
[2] J. L. Asensio, J. F. Espinosa, H. Dietrich, F. J. Canada, R. R. Schmidt, M. Martin-Lomas, S. Andre, H. J. Gabius, J. Jimenez-Barbero, *J. Am. Chem. Soc.* **1999**, *121*, 8995–9000.
[3] T. Haselhorst, J. F. Espinosa, J. Jimenez-Barbero, T. Sokolowski, P. Kosma, H. Brade, L. Brade, T. Peters, *Biochemistry* **1999**, *38*, 6449–6459.
[4] J. Klein, R. Meinecke, M. Mayer, B. Meyer, *J. Am. Chem. Soc.* **1999**, *121*, 5336–5337.
[5] V. V. Krishnan, *Curr. Anal. Chem.* **2005**, *1*, 307–320.
[6] B. Meyer, T. Peters, *Angew. Chem.* **2003**, *115*, 890–918; *Angew. Chem. Int. Ed.* **2003**, *42*, 864–890.
[7] M. Mayer, P. T. Lang, S. Gerber, P. B. Madrid, I. G. Pinto, R. K. Guy, T. L. James, *Chem. Biol.* **2006**, *13*, 993–1000.
[8] M. Mayer, T. L. James, *J. Am. Chem. Soc.* **2004**, *126*, 4453–4460.
[9] M. Mayer, T. L. James, *J. Am. Chem. Soc.* **2002**, *124*, 13376–13377.
[10] T. Maltseva, E. Usova, A. Eriksson, J. Milecki, A. Foldesi, J. Chattopadhayaya, *J. Chem. Soc. Perkin Trans. 2* **2000**, 2199–2207.
[11] M. Vogtherr, S. Limmer, *Magn. Reson. Chem.* **1998**, *36*, 901–906.
[12] S. Song, D. V. Velde, C. W. Gunn, R. H. Himes, *Biochemistry* **1994**, *33*, 693–698.
[13] Determination of solution conformation of receptor-bound ligands by NMR spectroscopy: A transferred nuclear-Overhauser-effect study of cyclophilin and a model substrate: L. T. Kakalis, I. M. Armitage in *Molecular Modeling: From Virtual Tools to Real Problems (ACS Symposium Series, Vol. 576)* (Eds.: T. F. Kumosinski, M. N. Liebman), ACS, Washington D.C., **1998**, pp. 29–44.
[14] G. K. Jarori, N. Murali, B. D. N. Rao, *Biochemistry* **1994**, *33*, 6784–6791.
[15] S. Neidle, *Nat. Prod. Rep.* **2001**, *18*, 291–309.
[16] J. B. Chaires, *Curr. Opin. Struct. Biol.* **1998**, *8*, 314–320.
[17] D. E. Wemmer, P. B. Dervan, *Curr. Opin. Struct. Biol.* **1997**, *7*, 355–361.
[18] J. Hunziker, *Chimia* **1996**, *50*, 248–256.
[19] D. Kahne, *Chem. Biol.* **1995**, *2*, 7–12.
[20] U. Pindur, M. Jansen, T. Lemster, *Curr. Med. Chem.* **2005**, *12*, 2805–2847.
[21] F. X. Han, N. Taulier, T. V. Chalikian, *Biochemistry* **2005**, *44*, 9785–9794.
[22] P. B. Dervan, B. S. Edelson, *Curr. Opin. Struct. Biol.* **2003**, *13*, 284–299.
[23] D. Renneberg, P. B. Dervan, *J. Am. Chem. Soc.* **2003**, *125*, 5707–5716.
[24] P. B. Dervan, *Bioorg. Med. Chem.* **2001**, *9*, 2215–2235.
[25] L. Wang, C. Bailly, A. Kumar, D. Ding, M. Bajic, D. W. Boykin, W. D. Wilson, *Proc. Natl. Acad. Sci. USA* **2000**, *97*, 12–16.
[26] F. G. Loontiens, P. Regenfuss, A. Zechel, L. Dumortier, R. M. Clegg, *Biochemistry* **1990**, *29*, 9029–9039.
[27] A. Abudaya, P. M. Brown, K. R. Fox, *Nucleic Acids Res.* **1995**, *23*, 3385–3392.
[28] S. Eriksson, S. K. Kim, M. Kubista, B. Norden, *Biochemistry* **1993**, *32*, 2987–2998.
[29] K. J. Breslauer, D. P. Remeta, W. Y. Chou, R. Ferrante, J. Curry, D. Zaunczkowski, J. G. Snyder, L. A. Marky, *Proc. Natl. Acad. Sci. USA* **1987**, *84*, 8922–8926.
[30] L. A. Marky, K. J. Breslauer, *Proc. Natl. Acad. Sci. USA* **1987**, *84*, 4359–4363.
[31] P. Peñalver, A. Samadi, P. Bosch, C. A. Hunter, C. Vicent, **2007**, unpublished results.
[32] J. N. Martin, E. M. Munoz, C. Schwergold, F. Souard, J. L. Asensio, J. Jimenez-Barbero, J. Canada, C. Vicent, *J. Am. Chem. Soc.* **2005**, *127*, 9518–9533.
[33] S. Di Micco, C. Bassarello, G. Bifulco, R. Riccio, L. Gomez-Paloma, *Angew. Chem.* **2006**, *118*, 230–234; *Angew. Chem. Int. Ed.* **2006**, *45*, 224–228.
[34] Since the chemical shifts of these key DNA proton resonances show rather distinct values to those of netropsin (**1**) and the sugar–oligoamide ligands **2**–**6**, selective irradiation of the internal or external region of DNA was possible (see Figure 16 in the Supporting Information). On this basis, and with the assumption of almost negligible spin diffusion, it should be possible to verify which part of the ligand is close to either area.
[35] With regard to netropsin (**1**), we first carried out a NOESY experiment in D_2O that allowed us to assign the ^1H NMR resonances in the free state. There is an incorrect assignment in reference [33]. Our assignment is in accordance with reference [38] and D. J. Patel, *Proc. Natl. Acad. Sci. USA* **1982**, *79*, 6424–6428).
[36] The normalization/standardization of the signal intensity was done relative to Py3 and Py5; both sets of data treatment render identical conclusions.
[37] M. W. Freyer, R. Buscaglia, D. Cashman, S. Hyslop, W. D. Wilson, J. B. Chaires, E. A. Lewis, *Biophys. Chem.* **2007**, *126*, 186–196.
[38] D. J. Patel, L. Shapiro, *J. Biol. Chem.* **1986**, *261*, 1230–1240.
[39] D. S. Goodsell, M. L. Kopka, R. E. Dickerson, *Biochemistry* **1995**, *34*, 4983–4993.
[40] K. Van Hecke, P. C. Nam, M. T. Nguyen, L. Van Meervelt, *FEBS J.* **2005**, *272*, 3531–3541.
[41] N. G. A. Abrescia, L. Malinina, J. A. Subirana, *J. Mol. Biol.* **1999**, *294*, 657–666.
[42] X. Chen, S. N. Mitra, S. T. Rao, K. Sekar, M. Sundaralingam, *Nucleic Acids Res.* **1998**, *26*, 5464–5471.
[43] L. Tabernero, N. Verdaguer, M. Coll, I. Fita, G. A. Vandermarel, J. H. Vanboom, A. Rich, J. Aymami, *Biochemistry* **1993**, *32*, 8403–8410.
[44] M. Coll, J. Aymami, G. A. Vandermarel, J. H. Vanboom, A. Rich, A. H. J. Wang, *Biochemistry* **1989**, *28*, 310–320.

[45] M. L. Kopka, C. Yoon, D. Goodsell, P. Pjura, R. E. Dickerson, *J. Mol. Biol.* **1985**, *183*, 553–563.
[46] M. Mobli, A. Almond, *Org. Biomol. Chem.* **2007**, *5*, 2243–2251.
[47] M. Avalos, R. Babiano, M. J. Carretero, P. Cintas, F. J. Higes, J. L. Jimenez, J. C. Palacios, *Tetrahedron* **1998**, *54*, 615–628.
[48] C. A. Hawkins, R. P. de Clairac, R. N. Dominey, E. E. Baird, S. White, P. B. Dervan, D. E. Wemmer, *J. Am. Chem. Soc.* **2000**, *122*, 5235–5243.
[49] R. P. L. de Clairac, B. H. Geierstanger, M. Mrksich, P. B. Dervan, D. E. Wemmer, *J. Am. Chem. Soc.* **1997**, *119*, 7909–7916.
[50] D. S. Pilch, N. Poklar, C. A. Gelfand, S. M. Law, K. J. Breslauer, E. E. Baird, P. B. Dervan, *Proc. Natl. Acad. Sci. USA* **1996**, *93*, 8306–8311.
[51] M. Gopal, M. S. Shahabuddin, S. R. Inamdar, *Proc. Indian Acad. Sci. Chem. Sci.* **2002**, *114*, 687–696.
[52] R. D. Wells, R. C. Grant, B. E. Shortle, C. R. Cantor, *J. Mol. Biol.* **1970**, *54*, 465–497.

Received: July 18, 2007
Revised: November 28, 2007
Published online: January 18, 2008

